Apoptosis (2026) 31:95
https://doi.org/10.1007/s10495-026-02261-x

REVIEW

Looking at the fraction with Annexin V$^+$ and propidium iodide$^+$: insights into cell death types from preclinical studies in solid and haematological cancers

Siti Nazihahasma Hassan[1,2] · **Farizan Ahmad**[1,2]

Received: 24 September 2025 / Accepted: 3 January 2026 / Published online: 11 March 2026

Abstract

Fluorescein isothiocyanate-conjugated Annexin V in combination with propidium iodide (PI) labelling is a widely used flow cytometric assay for quantifying apoptotic and necrotic cells in anticancer studies. However, increasing evidence suggests that double-positive cells, or the Annexin V$^+$/PI$^+$ fraction, may represent not only late apoptosis but also different modalities of regulated cell death, including necroptosis, pyroptosis, ferroptosis, and cuproptosis. By collating findings from preclinical studies across different cancer cells, this review highlights the need for consensus in interpreting Annexin V$^+$/PI$^+$ populations. In the absence of molecular and/or microscopy data, this fraction is more appropriately classified as undergoing 'late-stage cell death'. In short, establishing standardised interpretive criteria is crucial to enhance understanding, facilitate cross-study comparability, and improve the translational relevance of anticancer research.

Keywords Annexin v · Propidium iodide · Regulated cell death · Cancer cell death · Anticancer · Apoptosis

Introduction

Cancer, one of the major non-communicable diseases, is fundamentally characterised by deregulated apoptotic mechanisms and the uncontrolled proliferation of transformed cells. Although numerous mechanisms contribute to therapeutic resistance, evasion of cell death remains a central challenge in cancer treatment. Accordingly, the development and evaluation of agents capable of effectively triggering cell death, particularly through apoptosis, remains an active area of investigation. Apoptosis is an essential cellular process in mammalian systems, serving to eliminate transformed, damaged, infected, or dysfunctional cells, and plays a crucial role in post-embryonic development, adult tissue homeostasis, and the aetiology of multiple human disorders [1]. The term 'apoptosis', the first defined form of regulated cell death, was coined by Kerr et al. in 1972, marking the starting point in modern cell death research. However, studies on cell death can be traced back to the 1800s, with notable contributions from several pioneers in biomedical literature. In 1842, German anatomist Carl Vogt first proposed the concept of spontaneous cell death; in 1882, the Russian biologist Elie Metchnikoff described phagocytic cells engulfing dying cells; and in 1964, Lockshin and Williams introduced the term 'programmed cell death' [2–4]. In 2012, the Nomenclature Committee on Cell Death suggested the term 'regulated cell death' to indicate cases in which the initiation or execution is mediated by specific molecular machinery and can be inhibited by targeted pharmacological and/or genetic interventions. Meanwhile, the adjective 'programmed' refers to cell death that occurs in physiological contexts, such as during embryonic/post-embryonic development and tissue homeostasis, irrespective of the modality by which it is executed [5].

Fluorescein isothiocyanate (FITC)-conjugated Annexin V and propidium iodide (PI) co-labelling are commonly used to detect and quantify apoptotic and necrotic cells using flow cytometry in anticancer studies. Whilst Annexin V primarily marks apoptotic cells, double-labelling with

✉ Farizan Ahmad
farizan@usm.my

[1] Department of Neurosciences, School of Medical Sciences, Universiti Sains Malaysia, 16150 Kubang Kerian, Kelantan, Malaysia

[2] Hospital Pakar Universiti Sains Malaysia, 16150 Kubang Kerian, Kelantan, Malaysia

Annexin V and PI (Annexin V^+/PI^+) indicates compromised nuclear and plasma membranes in damaged or dead cells [6–8], often classified as late apoptosis [9–13] or apoptosis in general (in combination with Annexin V^+/PI^-) [14–16]. Nevertheless, accumulating evidence suggests that the Annexin V^+/PI^+ fraction may not represent the sole population of apoptotic cells. For example, under mild constant electrostimulation-induced pyroptosis in MCF7 breast cancer cells, indicated by an increased Annexin V^+/PI^+ fraction, the expression of both apoptosis- and pyroptosis-related genes was markedly elevated. Meanwhile, most genes associated with necrosis, necroptosis, and ferroptosis were downregulated, although a few were upregulated [17]. Co-treatment of SW620 colorectal cancer cells with cisplatin and quinoline-Val-Asp-difluorophenoxymethyl ketone (Q-VD-OPh), a pan-caspase inhibitor, still produced significant differences in Annexin V^+/PI^+ relative to untreated control or Q-VD-OPh alone [18]. Benzyloxycarbonyl-Val-Ala-Asp(OMe)-fluoromethylketone (z-VAD-FMK), a pan-caspase inhibitor, was reported to inhibit flubendazole-induced apoptosis and pyroptosis in U87 and U251 glioblastoma (GBM) cells. Flow cytometry showed negligible differences in the Annexin V-positive ($^+$) and Annexin V^+/PI^+ fractions compared with either the negative control or z-VAD-FMK alone [19]. In light of such findings, this review summarises the cell death modalities associated with the Annexin V^+/PI^+ fraction in preclinical anticancer studies and underscores the need for consensus in its interpretation.

Overview of flow cytometry

Flow cytometry is a rapid, reliable, and reproducible laser-based technique. It enables the detection of the plasma membrane, cytoplasmic, and nuclear antigens by labelling cells or particles with fluorochrome-conjugated antibodies or fluorescent dyes that specifically bind to components of interest [20]. The pioneering use of fluorescence detection to study biological molecules and processes is attributed to Gregorio Weber, a biochemist whose groundbreaking contributions in the 1940s and 1950s [21, 22]. In the late 1960s, Herzenberg and his colleagues adapted Fulwyler's design to develop an instrument capable of separating biological cells suspended in a conducting medium based on the presence or absence of fluorescently labelled molecules. This innovation marked the advent of the fluorescence-activated cell sorter (FACS). The licensing of Herzenberg's design by Becton Dickinson—which holds the trademark for the term 'FACS'—revolutionised cell sorting through flow cytometry technology [23–25].

In the early 1970s, Becton Dickinson Immunocytometry Systems introduced the first commercial FACS machines [25]. The main principle of flow cytometry is the interaction of fluorescent particles with a laser beam, resulting in light scattering and fluorescence emission [20]. The technique involves passing a single-file stream of cells or particles in suspension through a laser beam to measure their physical (i.e., optical) and chemical (e.g., antigen expression) features. As cells pass through the laser light, they absorb, refract (i.e., scatter), and emit light that is subsequently captured by an array of detectors. Forward scatter (FSC), the amount of light each cell scatters in the forward direction, reflects both the size and refractive index of the cell. Side scatter (SSC) indicates cell complexity, such as the presence of organelles, granules, and other intracellular features that cause light diffraction to the side [26].

It is noteworthy that apoptotic cells often display decreased FSC and increased SSC [6, 7, 27–30]. For example, the low FSC/high SSC subpopulation was Annexin V^+, whereas Namalwa Burkitt lymphoma cells with high FSC/low SSC were Annexin V-negative ($^-$). This shift in the FACS profile, observed only after 54 h, was consistent with the increased fractions of Annexin V^+ and Annexin V^+/ethidium bromide$^+$ cells, as well as nuclear condensation detected by Giemsa staining [6]. In addition, cell debris resulting from the disintegration of dying cells cannot be captured by FACS analysis, a limitation that can be circumvented by incorporating CountBright absolute counting beads [31].

Overview of the FITC-Annexin V/PI cell death assay

Phosphatidylserine (PS)-affinity assays with Annexin V enable the rapid, simple, and sensitive detection of apoptotic cells in suspension. PS externalisation on the outer membrane surface is a commonly used indicator of early apoptosis across diverse cell types and stimuli [32]. In contrast, PI, a deoxyribonucleic acid (DNA)-intercalating fluorochrome and analogue of ethidium bromide, is valued for its ease of use and high specificity for non-viable cells (damaged and dead cells). Intact plasma membranes exclude PI, and laser-excited fluorescence is detected only in the nuclei of dead cells [33, 34].

Annexin V, formerly named placental protein 4, was first reported by Inaba et al. [35] following its isolation from human placenta. In a separate study, Reutelingsperger et al. [36] isolated it from the umbilical cord by virtue of its anticoagulant activity and termed it vascular-anticoagulant-α. The subsequent cloning and sequencing of human Annexin V complementary DNA revealed its homology with the Annexin protein family, leading to its current designation [32].

Koopman et al. [6] pioneered the use of FITC-labelled Annexin V in flow cytometry to detect apoptotic cells

through binding to PS exposed on the plasma membrane. In the study, Annexin V^+ staining (green fluorescence) served as a specific marker for the early phase of apoptosis, characterised by intact cell membranes. At later stages of apoptosis, when membrane damage occurred, apoptotic cells were double-stained with Annexin V and ethidium bromide (a non-vital DNA stain) [6]. Notably, chromatin and nuclear condensation coincided with PS externalisation in apoptotic cells and preceded membrane damage, i.e., loss of plasma membrane integrity [6, 37]. In contrast, normal nuclear morphology was observed in Annexin V^- cells [37].

Meanwhile, Crissman and Steinkamp introduced PI as a safer alternative to ethidium bromide in the quantitative DNA staining of mammalian cells using flow microfluorometry, an early version of single-cell analysis by laser-excited fluorescence detection [38]. Krishan later developed a method using PI dissolved in isotonic saline, suitable for quantifying dead cells in a population, whilst a hypotonic PI solution leads to membrane destruction and rapid staining of nuclear DNA [34]. Further optimisation of PI labelling for nuclear DNA analysis revealed that the red fluorescence intensity of PI-DNA binding is influenced by sodium chloride concentration, whilst specificity is enhanced by enzymatic removal of ribonucleic acid [39–41].

It is noteworthy that Annexin V/PI fractions during camptothecin-induced apoptosis in Jurkat cells demonstrate a temporal progression. At 0 h, levels are negligible, with Annexin V^+/PI^- detected at 4 h and Annexin V^+/PI^+ at 22 h, which continues to increase at 48, 72, and 168 h [42]. Another time-course study revealed a highly consistent apoptotic index in Jurkat cells across Annexin V staining, nuclear morphology, PhiPhiLux caspase-3 activity, and terminal deoxynucleotidyl transferase dUTP nick end labelling (TUNEL), compared with Ramos Burkitt lymphoma and COLO205 colorectal [43]. In human lymphocytes undergoing radiation-induced apoptosis for 48 h, apoptotic cells measured by the comet assay closely match the sum of Annexin V^{++}/PI^- and Annexin V^+/PI^+ populations, with a near-perfect correlation ($r = 0.992$, slope = 0.97, and intercept = 1.5) [7]. In a separate investigation, the Annexin V^+/PI^+ population comprised a mixture of apoptotic and necrotic comets [44]. The Annexin V^+/PI^+ has, in certain publications, been labelled as "dead cells" [37, 45], "late apoptotic/secondary necrotic" [46], "necrotic" [47, 48], "late apoptosis and necrosis" [49], "late apoptosis and necrocytosis" [50], "post-apoptotic necrotic" [51], and "programmed (secondary) necrosis" [52]. Meanwhile, Annexin V^+/PI^- cells are classified as undergoing "primary apoptosis" [53]. As traditionally understood, the interpretation of the Annexin V/PI assay is shown in Fig. 1.

Beyond flow cytometry, Annexin V can detect apoptosis in adherent cells using time-lapse microscopy. Intriguingly, this approach enables live visualisation of cell death processes at different intervals of interest. It also captures the temporal sequence between Annexin V and PI or SYTOX Green staining uptake, given that membrane permeabilisation occurs relatively late during apoptosis. For example, in HT1080 fibrosarcoma cells or L929 fibroblasts stained

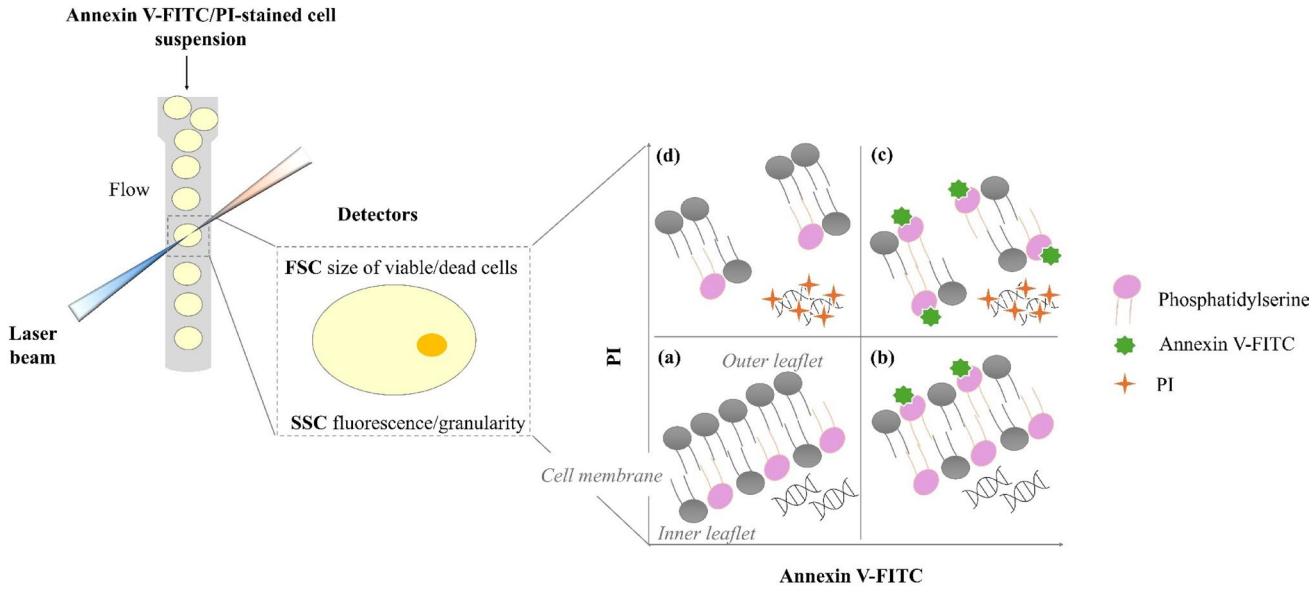

Fig. 1 Cartoon overview of FACS analysis with Annexin V-FITC (488 nm excitation/~530 nm emission, green) and PI (535 nm excitation/~617 nm emission, red) as fluorochromes. The fluorescence emitted by each stained cell is measured, allowing for discrimination between viable, apoptotic, and necrotic populations. In a typical quadrant analysis, cells are classified as **a** Annexin V^-/PI^-, indicating viable and undamaged cells; **b** Annexin V^+/PI^-, indicating cells in the early stages of apoptosis; **c** Annexin V^+/PI^+, indicating cells in the late stages of apoptosis where the plasma membrane integrity has been compromised; and **d** Annexin V^-/PI^+, indicating necrotic cells.
Adapted from El-Hajjar et al. [20] and Khalef et al. [126].

with Annexin V-Alexa Fluor 647 in combination with either PI or SYTOX Green, Annexin V positivity was consistently observed to precede double positivity. In contrast, membrane permeabilisation constitutes an early event in necrosis or necroptosis, with cells immediately becoming double-positive or directly positive for PI or SYTOX Green. Morphologically, these cells lacked blebbing and nuclear condensation [54]. Meanwhile, a separate protocol described the use of Annexin V-Alexa Fluor 647 and SYTOX Green for time-lapse imaging of pyroptosis [55]. The importance of temporal microscopy resolution in studying cell death is further underscored by observations that some apoptotic cells were Annexin V^-, yet exhibited membrane blebbing and nuclear condensation characteristic of apoptosis, later progressing to secondary necrosis [56]. Correspondingly, during camptothecin-induced apoptosis in HL60 cells, Annexin V binding occurred only after approximately 4 h, despite the apoptotic process of DNA cleavage and subsequent cellular disintegration being already well advanced by 3 h [29]. In studies investigating the interplay between apoptosis and ferroptosis, cells exhibiting blebbing phenotypes tended to die later than those that ruptured following swelling [57]. In particular, microscopy-based approaches enable the direct visualisation of apoptotic bodies, which are not readily detectable by classic Annexin V/PI flow cytometry analysis [30], but can be resolved using specialised acquisition and gating strategies [58, 59].

Additionally, it should be noted that PS externalisation is neither a universal event nor a unique phenomenon of apoptosis. For example, in response to apoptotic stimuli, limited PS exposure has been reported in T98G GBM, Daudi Burkitt lymphoma, and D32 glioma cells. In contrast, Annexin V binding was markedly higher in Jurkat cells [60]. Fadeel et al. (1999) demonstrated that PS externalisation occurs downstream of caspase activation in a cell-type-specific manner but is not an obligatory outcome of caspase activation. Meanwhile, caspase activation and nuclear changes are common features of apoptosis, irrespective of cell type or stimulus. Note that PS exposure was detected in Jurkat, CEM acute lymphoblastic leukaemia, and U937 lymphoma cells, but no changes were observed in HL60 acute myeloid leukaemia (AML), P39 myelodysplastic syndrome, or Raji Burkitt lymphoma [61]. On the other hand, Raji cells treated with compound 6i (a quinoline-3-carboxamide analogue) for 24 h showed a significant increase in the combined Annexin V^+ and Annexin V^+/PI^+ fractions. This was further supported by fluorescence microscopy and the elevated expression of apoptosis-related proteins, including caspase-3 and − 9, as well as cytochrome c [62]. PS exposure has also been reported in oncotic (early primary necrosis) JB6 cells, a subline of the Jurkat E human T-cell lymphoma. Notably, Annexin V^+/PI^- staining was observed by fluorescence microscopy and ultrastructural analysis using pre-embedding immunogold labelling and transmission electron microscopy (TEM) revealed PS at the outer leaflet of the intact plasma membrane, which retained its trilamellar structure [63].

Literature retrieval

Articles were retrieved from the ScienceDirect, Scopus, and Google Scholar databases to assess the types of cancer cell death linked to Annexin V^+/PI^+. The search strategy employed the following terms combined with appropriate Boolean operators (AND/OR): “anticancer”, “cytotoxicity”, “antitumour”, “cell death”, “cancer cells”, “apoptosis”, “necroptosis”, “pyroptosis”, “ferroptosis”, and “cuproptosis”. English-language publications from 2015 onwards were reviewed, accessible either as open access or through institutional subscriptions, with priority given to the most recent articles. Since the initial search predominantly retrieved studies on bioactive compounds or phytocompounds, additional searches were conducted for the known anticancer drugs, such as temozolomide (TMZ) and cisplatin, as well as for the five most common cancer types in males (lung, prostate, colorectum, stomach, and liver) and females (breast, lung, colorectum, cervix uteri, and thyroid) [64]. Further articles were incorporated in light of the author’s ongoing related research. Collectively, Table 1 includes only anticancer studies that reported flow cytometric quadrant data demonstrating an increased Annexin V^+/PI^+ fraction relative to untreated or vehicle controls. These studies also provided gene and/or protein expression analyses, with or without microscopy-based assays and cell death discrimination using pharmacological inhibitors and/or molecular inhibition via gene knockdown. Note that priority is given to protein expression data, unless only gene expression information was available. As a complement, Table 2 provides an overview of studies using qualitative methods in cell death detection. In contrast to Table 1, the studies in Table 2 were primarily microscopy-based analyses, performed either with or without Annexin V/PI staining and/or molecular assays. It aims to provide additional information on the types of cell death identified across different anticancer studies.

To find out whether the same phenomenon occurs in normal human cells exhibiting Annexin V^+/PI^+, relevant literature was identified through searches in the Scopus and Google Scholar databases. The search was conducted without year preference using multiple keyword combinations, including but not limited to: “Annexin V and PI”, “cell death”, AND/OR “normal cells”. In addition to the initial database search, SpringerLink was also examined for

Table 1 Summary of selected anticancer studies with increased Annexin V^+/PI^+ fraction

In vitro cancer model	Treatment	Specified mode of cell death	Methodologies			Other/common parameters		Reference
			Western blot, RT-qPCR, and/or other assays (related molecules)		Microscopy description			
			↑	↓		↑	↓	
HepG2 liver cells	Copper(II) Schiff base complex	Apoptosis	Caspase-3 and −5 activities, and GSDME-N/GSDME ratio			Sub-G1 fraction, ROS	ΔΨm	[72]
U87 and U251 GBM cells	Platycodin D (triterpenoid saponin)	Apoptosis	Cleaved caspase-3, BAX	BCL2				[73]
MCF7 breast cells	Berberine-zinc oxide conjugated chitosan NPs	Apoptosis	Caspase-8 and −9 activity, *BAX*	*BCL2*	AO/PI: early (bright green) and late apoptosis (orange), with chromatin condensation, membrane blebbing, and apoptotic bodies; Hoechst 33,342: intense blue fluorescence	Sub-G1 fraction, ROS		[74]
AGS gastric and H727 lung cells	3-Carene (a naturally occurring bicyclic monoterpene from *Piper nigrum*)	Apoptosis	*BAX*, *cytochrome c*, and *caspase-3*	*BCL2*	Hoechst 33,258: irregular nuclear staining with chromatin condensation and nuclear fragmentation	Sub-G1 fraction		[75]
EJ138 bladder cells	Genistein (a 7-hydroxyisoflavone)	Apoptosis	*Caspase-3* and *−9*					[15]
U937 lymphoma cells	Erbium oxide NPs	Apoptosis	*BCL2*	*TP53*, *ND3*	Comet assay: DNA tail formation	ROS	ΔΨm	[9]
MCF7 breast and HepG2 liver cells	Metformin	Apoptosis	*BAX*, *TP53*	*BCL2*		Sub-G1 fraction, GSH		[45]
Distinct *TP53* statuses: HCT116 (wild-type), HT29 (mutated), and SW1417 (deleted) colorectal cells	11-keto-β-boswellic acid (a bioactive constituent of olibanum extract)	Apoptosis	Cleaved caspase-3, *BAK1*, *BCL-XL*, and BAX	BCL2	DAPI staining: DNA shrinkage in the nuclei	Sub-G1 fraction, DNA fragmentation		[76]
DOHH-2 and RL lymphoma cells	Anlotinib	Apoptosis	Cleaved caspase-3 and PARP, BAX, BAK, p-p53 (Ser15), and p53	MCL1		γH2AX		[77]
NB4 AML cells	Cytarabine	Apoptosis	*BAX*/*BCL2* ratio, *TP53*, and *CDKN1A*					[16]

Table 1 (continued)

In vitro cancer model	Treatment	Specified mode of cell death	Methodologies			Other/common parameters		Reference
			Western blot, RT-qPCR, and/or other assays (related molecules)		Microscopy description			
			↑	↓		↑	↓	
OVCAR-8 ovarian cells	Carboplatin	Apoptosis	Caspases 3/7, 8, and 9 activities					[78]
U251 and C6 GBM cells	tdIHG co-delivers TMZ and DSF, with oral copper supplementation	Apoptosis, ICD	Calreticulin, HMGB1, CXCL10, and CHOP			γH2AX, ATP, $CD8^+$ T cell chemotaxis, and mtROS		[79]
MDA-MB-231 breast cells	DMOCPTL (a parthenolide derivative)	Apoptosis, ferroptosis	Cleaved caspase-9, -3, and PARP, BAX, and cytochrome c	BCL2, BCL-XL, and GPX4		Fe^{2+}, ROS		[80]†
MDA-MB-231 breast cells	Stannum complex C5	Apoptosis, pyroptosis	Cleaved caspase-3, IL-18, IL-1β, NLRP3, and GSDME-N		Phase contrast: cytoplasmic swelling; Hoechst33342: wrinkled nuclei; Comet assay: DNA tail formation	LDH, ROS	ΔΨm	[81]
AtT20, GH3, and MMQ Pit-NET cells	DSF	Cuproptosis	DLAT oligomerisation, HSP70	Fe–S cluster proteins, lipoylation of DLAT and DLST				[82]†
RMCCA-1 CCA cells	Kaempferol + z-VAD-FMK + LCL-161 (a cIAP1/2 inhibitor)	Necroptosis	p-MLKL, calreticulin, and HMGB1					[83]†
H2452, H28, and 211 H MPM cells	Deoxypodophyllotoxin (a natural flavonolignan-derived MTA)	Necroptosis	p-RIPK1, p-RIPK3, p-MLKL, and TNF-α		TEM: plasma membrane rupture, cytoplasmic translucency, organelle swelling, and numerous autophagosomes			[84]†‡
U87 GBM cells	Chelerythrine (a benzophenanthridine alkaloid)	Necroptosis	Cleaved caspase-3 and PARP, p-RIPK1/RIPK1, p-RIPK3/RIPK3, and p-MLKL/MLKL ratios, TNF-α			ROS, mtROS	ATP, ΔΨm	[85]†‡
4T1 breast cells	Sodium oxamate NPs	Pyroptosis	Cleaved caspase-1, calreticulin, GSDMD-N, IL-1β, and HMGB1		Phase contrast: cell swelling with big bubbles	ATP, LDH, and ROS		[86]

Table 1 (continued)

In vitro cancer model	Treatment	Specified mode of cell death	Methodologies		Other/common parameters		Reference
			Western blot, RT-qPCR, and/or other assays (related molecules)	Microscopy description			
			↑ ↓		↑	↓	
U87 GBM cells	Biomimetic cisplatin-polyphenol nanocomplex	Pyroptosis	Cleaved caspase-3, calreticulin, GSDME-N, and HMGB1	SEM: cell swelling, plasma membrane bubbling, and pore formation	LDH	GSH	[87]
A549 and H1299 NSCLC cells	EEBR (an alkaloid compound)	Pyroptosis	Caspase-1, IL-18, IL-1β, GSDMD-N, NF-κB, and NLRP3	TEM: Ruptured morphology; Hoechst 33,342/PI: apoptotic and necrotic cells	LDH		[88]†

AO – Acridine orange; BCL-XL – B-cell lymphoma extra large; cIAP1/2 – Cellular inhibitor of apoptosis proteins 1 and 2; CCA – Cholangiocarcinoma; CXCL10 – C-X-C motif chemokine ligand 10; CHOP – C/EBP homologous protein; CDKN1A – Cyclin dependent kinase inhibitor 1 A; DAPI – 4′,6-diamidino-2-phenylindole; DSF – Disulfiram; DLST – Dihydrolipoamide S-succinyltransferase; EEBR – 9-(2-ethoxyethoxy)-10-methoxy-5,6-dihydro- [1, 3]dioxolo[4,5-g]isoquinolino[3,2-]isoquinolin-7-ium bromide; GSH – Glutathione; GPX4 – Glutathione peroxidase 4; HSP70 – Heat shock protein 70; MCL1 –MCL1 apoptosis regulator, BCL2 family member; MPM – Malignant pleural mesothelioma; MTA – Microtubule-targeting agent; NSCLC – Non-small cell lung carcinoma; NLRP3 – NLR family pyrin domain-containing 3; NPs – Nanoparticles; ND3 – NADH dehydrogenase subunit 3; PitNET – Pituitary neuroendocrine tumour; p-MLKL – Phosphorylated MLKL; TP53 – Tumour protein p53 gene; tdIHG –Intranasal ion-sensitive in situ gel; p-p53 Ser15 – Phosphorylated p53 at serine-15; γH2AX – Phosphorylated histone variant H2AX; RT-qPCR – Reverse transcription quantitative polymerase chain reaction; SEM – Scanning electron microscopy. Symbols: ↑ indicates an increase compared with the untreated or vehicle controls, whereas ↓ represents a decrease; † marks studies employing one or more pharmacological inhibitors of cell death, whereas ‡ denotes molecular inhibition achieved through gene knockdown.

further relevant articles. With recent advances in artificial intelligence tools, the free version of ChatGPT was used to retrieve supplementary literature using the query: 'Can you help me find the article that uses Annexin V/PI staining in normal cells?'. However, the search yielded varying query results at different times, only three of which ([65–67]) were included after reviewing the full text. Overall, searches across multiple scholarly databases are recommended for more comprehensive literature retrieval. Table 3 summarises the mechanistic interpretation of the Annexin V/PI assay in normal cells. In all tables, blank cells indicate that data are unavailable, and as not all data were extracted, further information can be found in the cited reference.

Annexin V^+/PI^+ populations across cancer models: evidence from preclinical studies

Out of 36 cancer sites, a total of 13 distinct cancer types were represented in Table 1, encompassing 27 cell lines—22 of human origin and five rodent. Of these, 23 were derived from solid tumours and four from haematological malignancies. Across the 21 studies included, apoptosis was the most common form of cell death (n = 11), followed by necroptosis and pyroptosis (each n = 3), and cuproptosis (n = 1). Meanwhile, apoptosis in combination with immunogenic cell death (ICD), ferroptosis, or pyroptosis was reported only once. Of which, five emerging forms observed in anticancer studies are illustrated in Fig. 2. ICD, on the other hand, is not regarded as an exclusive or independent mode of cell death, as it can occur in multiple types of regulated cell death, including apoptosis, cuproptosis, ferroptosis, necroptosis, and pyroptosis. ICD represents a form of regulated cell death that elicits an immune response through the release of damage-associated molecular patterns (DAMPs) [3]. Several DAMPs have been mechanistically linked to the perception of regulated cell death as immunogenic, including calreticulin, adenosine triphosphate (ATP), high-mobility group box 1 (HMGB1), heat shock proteins, type I interferon, cancer cell-derived nucleic acids, and annexin A1 [3, 68]. In a review focused on liver injury and hepatocyte death, various pro-inflammatory mediators released from mitochondria, collectively termed mito-DAMPs, include cytochrome c, mitochondrial DNA, mitochondrial reactive oxygen species (mtROS), ATP, cardiolipin, and carbamoyl phosphate synthetase 1 [69].

It is worth noting that mitochondrial apoptosis and endoplasmic reticulum stress exert mutually amplifying effects on the anti-tumour immune response, resulting in the release of large amounts of DAMPs, leading to ICD [70]. Furthermore, the immunogenicity of cell death was shown to represent the default outcome of apoptosis, which is actively repressed by the same machinery. Specifically, the unconventional autophagic pathway activated by BCL2 antagonist/killer (BAK) inhibits ATP release during apoptotic cell death, whereas ATP functions as a molecular mediator that induces interleukin-1 beta (IL-1β) secretion [71]. Taken together, whilst potential variations due to differences in

Table 2 Summary of selected studies that determine different cell death types using qualitative methods, substantiated with or without Annexin V/PI and molecular assays

In vitro cancer model	Treatment	Specified mode of cell death	Methodologies				Other/common parameters		Reference
			Flow cytometry	Western blot, RT-qPCR, and/or other assays (related molecules)		Microscopy description	↑	↓	
				↑	↓				
MDA-MB-231 breast cells	Ethyl acetate fraction from *Allium sativum* L.	Apoptosis	Annexin V^+/PI^+			Hoechst 33,258: nuclear and chromatin condensation; AO/EB: early apoptosis was marked by nuclear condensation with green cytoplasm, and late apoptosis with orange cytoplasm	ROS	ΔΨm	[89]
BGC-823 gastric cells	Naringenin hydrazone derivatives	Apoptosis	Annexin V^+/PI^+			AO/EB: early apoptotic cells appeared green, whereas late apoptotic cells were orange-red, with features such as shrinkage, enhanced fluorescence intensity, chromatin condensation, and nuclear fragmentation	ROS		[90]
PA-1 ovarian cells	Platinum NPs	Apoptosis	Annexin V^+/PI^+			AO/EB: chromatin condensation; green, yellow, and reddish-orange represent viable, early apoptotic, and late apoptotic cells, respectively	Sub-G1 fraction		[91]†
HCT116 colorectal cells	Cisplatin	Apoptosis, ferroptosis			GPX activity	TEM: mitochondria are smaller, less tubular, have darker membranes, and disrupted cristae	ROS	GSH	[92]†
MOLM-14 AML cells	APR-246	Ferroptosis		SLC7A11		TEM: mitochondrial membrane rupture, reduced cristae	Lipid peroxidation, cystine uptake	GSH	[93]†
U87, U251, and U118 GBM cells	RSL3	Ferroptosis		TF, TFR, FT, FPN, and SIRT1	GPX4	FerroOrange: increased intracellular Fe^{2+}	LDH, MDA		[94]†
HT29 colorectal cells	Resveratrol	Ferroptosis			GPX4, SLC7A11	TEM: mitochondrial shrinkage, disappearance of cristae; co-administration with ferrostatin-1 reverses the observed effects	ROS, MDA, and Fe^{2+}	ΔΨm	[95]†
HSC3 and SCC4 OSCC cells	Acetylshikonin (a naphthoquinone derivative)	Ferroptosis, necroptosis	Annexin V^-/PI^+	p-RIPK1, p-RIPK3, and p-MLKL	GPX4	DAPI: nuclear changes; TEM: HSC3 cells showed mitochondrial swelling and endoplasmic reticulum disruption	ROS	ΔΨm	[96]†

Table 2 (continued)

In vitro cancer model	Treatment	Specified mode of cell death	Methodologies				Other/common parameters		Reference
			Flow cytometry	Western blot, RT-qPCR, and/or other assays (related molecules)		Microscopy description	↑	↓	
				↑	↓				
MDA-MB-231 breast cells	M@P under light irradiation	Ferroptosis, pyroptosis		Cleaved caspase-1, calreticulin, HMGB1, IL-18, IL-1β, and GSDMD-N	GPX4	AO: lysosomal dysfunction	ATP, LDH, ROS, and MDA	GSH	[97]
HuCCT1 CCA cells	Plumbagin	Pyroptosis		Cleaved caspase-1, IL-18, IL-1β, NLRP3, and GSDMD-N		SEM: membrane pores (varied sizes), cell swelling and bubble	LDH, ROS		[98]
OVCAR3 ovarian cells	CBL0137 (a small-molecule inhibitor)	Pyroptosis		Cytochrome c, cleaved caspase-3 and −9, GSDME-N, and BAX		Phase-contrast microscopy: membrane ballooning; TEM: disrupted cell membrane integrity, enlarged nucleus, decreased nuclear content, and lack of mitochondrial cristae	LDH, ROS		[99]†

EB – Ethidium bromide; M@P – A multifunctional pH-responsive theranostic nanoplatform, composed of aggregation-induced emission photosensitiser MTCN-3 and immunoadjuvant Poly(I: C), encapsulated in amphiphilic polymers; FT – Ferritin; FPN – Ferroportin; MDA – Malondialdehyde; OSCC – Oral squamous cell carcinoma; RSL3 – RAS-selective lethal compound 3; SIRT1 – Silent information regulator 1; SLC7A11 – Solute carrier family 7 member 11; TF – Transferrin; TFR – Transferrin receptor

death stimuli and cell-intrinsic factors cannot be excluded, increases in ROS (intracellular and mitochondrial), LDH, and the sub-G1 fraction, as well as DNA fragmentation and loss of mitochondrial membrane potential (ΔΨm), are commonly observed and associated with the cell death processes. Nevertheless, these parameters do not specifically define the mode of cell death. Tables 2 and 3 are considered as supplementary information; however, those with Annexin V^+/PI^+ also indicate alternative cell death pathways.

Discussion and outlook

As evidenced in Table 1–3, whilst Annexin V^+ cells can be considered to be undergoing apoptosis, it is clear that Annexin V^+/PI^+ fraction may not solely indicate the late stages of apoptosis. On the other hand, Annexin V negativity may indicate the involvement of non-apoptotic cell death pathways; however, this is not necessarily the case. Whilst some studies reporting ferroptotic and pyroptotic cell death did not assess Annexin V staining, it is important to note that Annexin V can bind to internal PS following membrane rupture, and distinct modes of regulated cell death may therefore exhibit Annexin V positivity. For example, ferroptosis did not induce PS exposure on the outer leaflet of the plasma membrane before loss of membrane integrity, resulting in an Annexin V^- and Annexin V^+/7-aminoactinomycin D $(7\text{-AAD})^+$ profile [104]. In particular, Annexin V/PI flow cytometry analysis alone is insufficient to define specific regulated cell death modalities. Nevertheless, its simplicity and quantitative output make it valuable for initial screening of the magnitude of cell death induction in experiments.

It also warrants consideration that although PI is the most commonly used viability exclusion dye, other fluorophores with DNA-binding properties can also be used. Examples include 7-AAD [105], ethidium homodimer [106], and DAPI [31, 107], which sometimes display better performance than PI. In particular, the broad emission spectrum of PI substantially overlaps with those of FITC and phycoerythrin (PE) [108], leading to bleed-through of FITC or PE fluorescence into the PI channel or secondary excitation of PI. On the other hand, the emission spectrum of 7-AAD does not overlap with that of FITC. Unlike PI, 7-AAD did not leech from permeabilised, fixed spermatozoa, with fluorescence remaining stable for up to 4 h post-staining [109]. In another study, Annexin V-FITC/7-AAD was used to detect apoptosis in lymphocyte subsets without interference from residual erythrocytes. Notably, a comparison between

Table 3 Summary of selected studies with increased Annexin V^+/PI^+ fraction involving normal cells

Normal cell type	Treatment	Specified mode of cell death	Methodologies				Other/common parameters		Reference
			Western blot, RT-qPCR, and/or other assays (related molecules)		Microscopy description	Remarks			
			↑	↓			↑	↓	
Primary human dermal fibroblasts	UVB irradiation	Apoptosis	Cleaved PARP			No evidence of ferroptosis, necroptosis, parthanatos, or AIF translocation			[66]†
HUVEC	TNF-α stimulation	Apoptosis	Cytochrome c, cleaved caspase-3, caspase 3/7 activity, and *DNM1L*		MitoTracker Red: altered mitochondrial morphology, with shorter branches and smaller networks		mtROS	ΔΨm	[67]
HUVEC	Angiotensin II	Apoptosis	Cleaved caspase-3 and −9, BAX, BAD, and cytochrome c	BCL2	Hoechst33342: nuclear shrinkage/chromatin condensation; AO/EB: live cells (green), early apoptosis (yellow), late apoptosis (orange), and necrosis (red)		ROS, LMP	ΔΨm	[100]
Primary human gingival fibroblasts	Curcumin	Apoptosis					ROS	ΔΨm	[101]
HUVEC	Starved conditions + TNF-α stimulation	Apoptosis	Cleaved caspase-3		DAPI: nuclear fragmentation				[65]
Primary human dental pulp fibroblasts	LPS stimulation	Ferroptosis, PANoptosis	Caspase-1, cleaved caspase-8, cleaved GSDMD, CCL2, CCL5, IL-6, IL-18, IL-1β, NLRP3, p-MLKL, RIPK3, and TNF-α	GPX4, *SLC7A11*, *FTH1*, and *FPN1*			$Fe2^+$, MDA, ROS	GSH	[102]
R28 retinal precursor cells	Glutamate	Necroptosis	Cleaved caspase-1, RIPK1, RIPK3, p-MLKL, NLRP3, IL-1β, *TNF-α*, and *IL-6*		Hoechst/PI: time-dependent PI uptake; TEM: cell swelling, plasma membrane rupture		LDH, ROS	GSH	[49]†
Primary human gingival fibroblasts	Adenovirus type 4 containing full-length NLRP6	Pyroptosis	Cleaved caspase-1, IL-18, IL-1β, and GSDMD-N		TEM: membrane rupture, chromatin margination and condensation, nuclei and mitochondria remain intact, but are swollen	Ac-YVAD-cMK (caspase-1 inhibitor) reduced the Annexin V^+/PI^+ fraction			[103]†

AIF – Apoptosis-inducing factor; BAD – BCL2-associated agonist of cell death; CCL2/5 – C-C motif chemokine 2/5; DNM1L – Dynamin 1-like; FTH1 – Ferritin heavy chain 1; HUVEC – Human umbilical vein endothelial cells; LPS – Lipopolysaccharide; LMP – Lysosomal membrane permeabilisation; UVB – Ultraviolet B

PI and 7-AAD in 25 different mononuclear cell samples showed a strong correlation for both apoptosis ($r = 0.88$, $P < 0.001$) and necrosis ($r = 0.99$, $P < 0.001$) [110]. In addition, one group compared Annexin V-Alexa Fluor 488/PI with Annexin V-Alexa Fluor 488/TO-PRO-3 in primary human airway epithelial cells, showing that TO-PRO-3 enables finer discrimination of cell death states than PI [30]. Alternatively, Annexin V conjugated with allophycocyanin

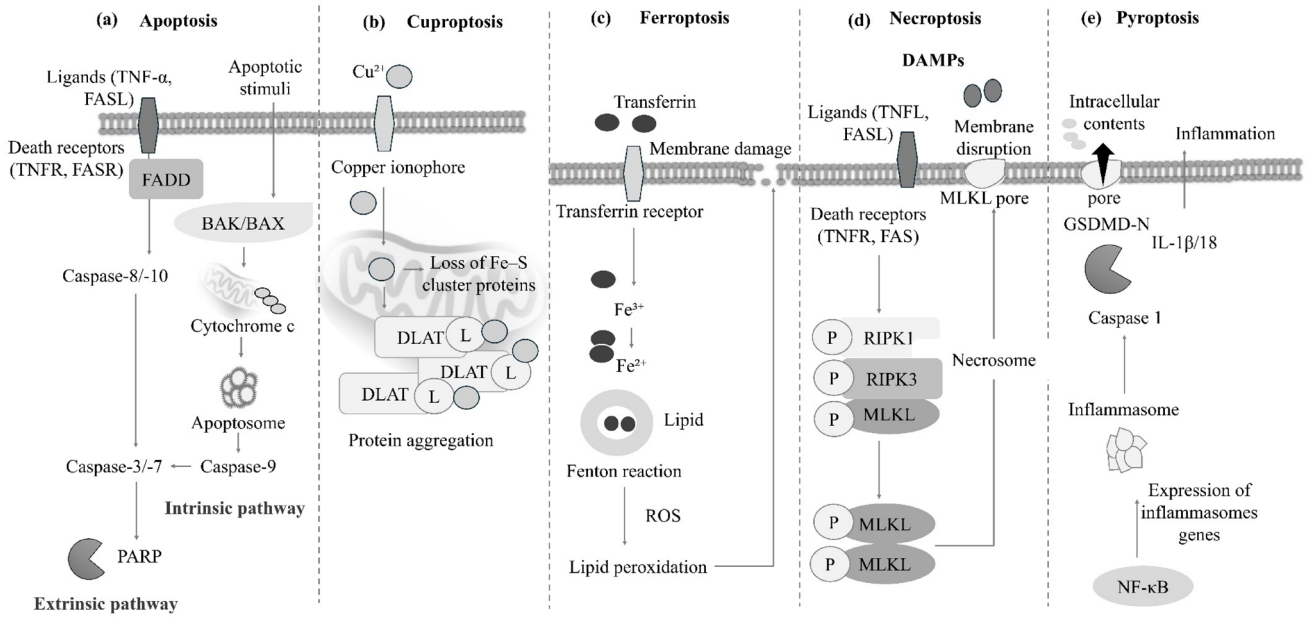

Fig. 2 Schematic representation of emerging regulated cell death mechanisms in anticancer research. **a** A tightly regulated process of cellular breakdown initiated via the extrinsic pathway (death ligands binding to death receptors) and/or the intrinsic pathway (BCL2-family regulation of mitochondria), involving cytochrome c release and caspase activation. **b** Triggered by copper accumulation, which results in mitochondrial stress due to the aggregation of lipoylated mitochondrial enzymes and the loss of Fe–S cluster proteins. **c** An iron-dependent process characterised by intracellular GSH depletion and decreased GPX4 activity, resulting in lipid peroxide accumulation and increased ROS production. **d** A regulated form of necrosis triggered by death receptors such as TNFR1, the RIPK1 binds to RIPK3 to form a necrosome, which activates MLKL. The oligomeric form of MLKL is translocated from the cytosol to the plasma membrane, leading to the formation of pores and subsequent rupture, releasing DAMPs that promote inflammation. **e** Triggered by the activation of inflammasomes, cytoplasmic complexes that sense danger signals and initiate a caspase-1-mediated cleavage of GSDMD, leading to pore formation and the release of proinflammatory cytokines such as IL-1β and IL-18. Abbreviations: BCL2 – BCL2 apoptosis regulator; BAX – BCL2 associated X, apoptosis regulator; Cu^{2+} – Cupric iron; DLAT – Dihydrolipoyl transacetylase; FADD – Fas-associated protein with death domain; FASL – Fas ligand; FASR – Fas receptor; Fe^{2+} – Ferrous iron; Fe^{3+} – Ferric iron; Fe–S – Iron–sulphur; GSDMD – Gasdermin D; GSDMD-N – N-terminal fragment of GSDMD; L – Lipoylation; MLKL – Mixed lineage kinase domain like pseudokinase; NF-κB – Nuclear factor kappa-light-chain-enhancer of activated B cells; P – Phosphorylation; PARP – Poly(ADP-ribose) polymerase; ROS – Intracellular ROS; RIPK1/3 – Receptor interacting serine/threonine kinase 1/3; TNF-α – Tumour necrosis factor-alpha; TNFR – Tumour necrosis factor receptor; TNFL – TNF ligand.
Adapted from Park et al. [3].

can be used in combination with DAPI [111–113], providing better separation of emission spectra. Notwithstanding, a double positive result with other fluorophore combinations may also indicate distinct modalities of cell death. For instance, PANoptosis was demonstrated by Annexin V-PE and 7-AAD positivity, involving the activation of apoptosis, necroptosis, and pyroptosis pathways [114].

Further understanding of flow cytometry-based apoptosis quantification, including filter selection, compensation controls, and troubleshooting, can be found in protocol-oriented articles [31, 115–118]. In parallel, various sources provide methods for distinguishing between different forms of regulated cell death, yet no ready-to-use assay can simultaneously identify them. One example is a protocol article describing phase-contrast microscopy approaches used to differentiate between apoptosis, necrosis, necroptosis, and ferroptosis, incorporating selective inhibitors of these cell death types [119]. Another study presents a flow cytometry assay to detect apoptosis, necroptosis, and RIPK1-mediated apoptosis at once [120]. Meanwhile, various groups of scientists have provided detailed coverage of the molecular mechanisms and/or morphological characteristics of distinct types of cell death, including [3, 68, 121–125], as well as the advantages and limitations of different cell death assays [126]. Notably, inhibition of necroptosis by necrostatin-1 may affect apoptosis, e.g., it suppresses etoposide-induced caspase activation and ripoptosome formation [127]. Likewise, necrostatin-1 reduced IL-1β-induced cleaved caspase-3 protein expression and Annexin V^+/PI^+ fraction in chondrocytes [128]. Necrostatin-1 also suppressed traumatic brain injury-induced autophagy and apoptosis in vivo [129]. In addition, whilst z-VAD-FMK rescues only HepG2 cells from apoptosis, necrostatin-1 reverses both apoptosis and necroptosis [130]. On the contrary, necrostatin-1 allows discrimination between apoptotic and necroptotic cells identified by Annexin V^+/PI^- staining [131].

In the second place, differences may exist between cell types, regardless of whether they are cancerous or normal

(cell-intrinsic factors). For example, apoptosis inhibition in human dermal fibroblasts by Q-VD-OPh does not trigger compensatory cell death via necroptosis or ferroptosis [66]. Mesenchymal stem cells undergo RIPK1 kinase-dependent apoptosis in response to a single low dose of TNF. However, inhibition of caspase activity with z-VAD-FMK shifts cell death towards necroptosis [132]. In a separate study, necroptosis was found to be tissue- and context-specific, with RIPK3 able to drive inflammation independently of MLKL in certain tissues [133]. On the other hand, MLKL sensitises human dermal fibroblasts to UVB-induced apoptosis, whereas RIPK3 exerts a protective effect, with no evidence of necroptosis activation [134]. Meanwhile, in HepG2 liver cancer cells, CBL0137 induces both apoptosis and necroptosis, with apoptosis being the dominant pathway. Notably, necroptosis inhibition with necrosulfonamide (MLKL inhibitor), necrostatin-1 (RIPK1 inhibitor), or GSK872 (RIPK3 inhibitor) demonstrated no changes, whereas caspase inhibition with z-VAD-FMK or z-IETD-FMK (caspase-8 inhibitor) significantly reduced CBL0137-induced cytotoxicity [50]. Additionally, GPX4 inhibition by (1 S, 3 R)-RSL3 induced HT1080 fibrosarcoma cell death that is partially prevented by z-VAD-FMK and Q-VD-OPh [57].

It is worth noting that apoptotic cells can undergo secondary necrosis if they are not efficiently scavenged by phagocytes (e.g., macrophages), a scenario common in cell culture settings [135]. Mechanistically, secondary necrosis occurs downstream of the mitochondrial apoptotic pathway and caspase-3 activation. In response to the anticancer agent etoposide (topoisomerase II inhibitor), cells expressing deafness, autosomal dominant 5 (DFNA5) progressed to secondary necrosis, but disassembled into small apoptotic bodies when DFNA5 was knocked out. Active caspase-3 cleaves DFNA5 at Asp270 to generate the necrotic DFNA5-N fragment, which permeabilises the plasma membrane by forming large pores, causing osmotic lysis of the cell and releasing cellular contents, including proinflammatory mediators. Time-lapse microscopy revealed membrane blebbing that progressed to cytoplasmic swelling (ballooning) in *DFNA5*$^{+/+}$ cells, whilst flow cytometric analysis showed prominent Annexin V^{-}/PI^{+} and Annexin V^{+}/PI^{+} populations [52]. Moreover, deletion of the autophagy genes autophagy-related 5 and beclin 1 impaired the clearance of apoptotic cells without affecting the occurrence of apoptosis. In the study, autophagy-deficient embryoid body cells exhibited almost no Annexin V staining despite caspase-3 activation, TUNEL positivity, and ultrastructural characteristics of apoptosis [136].

Less immunogenic than necroptosis, pyroptosis, or other regulated cell death pathways, apoptosis has historically been the preferred approach in anticancer strategies. Nonetheless, it may still trigger proinflammatory signalling molecules, such as IL-1, under certain conditions [123]. Currently, other regulated cell death modalities are being increasingly considered for their potential to suppress tumour growth. For instance, knockdown of *GPX4* by small interfering RNA induces ferroptosis and apoptosis in breast cancer cells [80]. Apoptosis and ferroptosis act in concert in APR-246 (a small molecule that restores wild-type p53 function in *TP53*-mutant cells)-induced killing of U937 lymphoma cells, but not of HT29 colorectal cancer cells [137]. In a different study, phototherapy-induced pyroptosis and ferroptosis triggered ICD, releasing tumour antigens that promoted RAW 264.7 cell migration [97]. Conversely, another group reported that ferroptosis in cancer cells does not constitute an immunogenic form of cell death, despite the release of cytokines, chemokines, DAMPs, and interferons. Moreover, ferroptosis appears less effective at controlling tumour growth than apoptosis and necroptosis, and it diminishes the immunogenicity of apoptosis [104]. In a murine breast cancer model, tumour cells undergo necroptosis in necrotic regions, which promotes metastasis [138].

Overall, cell death is a complex biological process, and understanding its mechanisms is fundamental to translational pharmacology. In particular, identifying the optimal cell death modalities for different tumour types is crucial for achieving the desired anticancer efficacy and advancing precision oncology. However, the question remains whether anticancer agents, alone or in combination, trigger multiple regulated cell death pathways and whether co-activation enhances therapeutic outcomes compared with apoptosis alone. Notably, a 2023 review by the Nomenclature Committee on Cell Death highlighted that many studies have yet to address the interplay between intrinsic and extrinsic apoptotic pathways, their overlap with other forms of regulated cell death, or the compensatory activation of alternative death pathways upon inhibition of apoptosis [1]. Additionally, though beyond the scope of this narrative, flow cytometric analysis of cell death from independent repeats (biological replicates) is reported as mean (standard deviation) for normally distributed data. In contrast, using the standard error of the mean reduces the apparent size of error bars but masks the true variability [139].

Limitations

The present narrative review did not address or mechanistically link each type of cell death in detail but rather aimed to shed light on different death modalities associated with Annexin V^{+}/PI^{+} populations among distinct cancer cells, as well as those of normal origin. Moreover, only several cell death types are highlighted, although 17 distinct cell death

modalities have been described [3]. Whilst this review was limited to anticancer studies, the Annexin V/PI flow cytometry assay is widely applied in studies of cell death-related non-communicable diseases, including cardiovascular and neurological conditions. For example, acute ischemic stroke [140] and Alzheimer's disease [141].

Conclusion

There is no clear consensus on the mode of cell death represented by the Annexin V^+/PI^+ population. This fraction cannot be assumed to reflect apoptosis alone. Follow-up experiments, including morphological observation, analysis of cell death-associated markers via RT-qPCR or immunoblotting, and/or time-lapse imaging, are necessary for reliable identification of apoptosis or other regulated cell death modalities. Where feasible, inclusion of selective cell death inhibitors can provide further insights into the underlying mechanisms of cell death. In the absence of such supporting evidence, it may be appropriate to classify the Annexin V^+/PI^+ population as 'late-stage cell death'. Whilst, to our knowledge, data on normal cells are scarce, Annexin V^+/PI^+ staining has likewise been associated with distinct modes of cell death.

Acknowledgements The authors thank Universiti Sains Malaysia for the Bridging Grant (R501-LR-RND003-0000001456-0000) and the Post-Doctoral Fellowship.

Author contributions **SNH** : Conceptualised, wrote, edited, and reviewed the paper. **FA** : Supervised, conceptualised, edited, and reviewed.

Funding Open access funding provided by The Ministry of Higher Education Malaysia and Universiti Sains Malaysia. Not applicable.

Data availability No datasets were generated or analysed during the current study.

Declarations

Ethics approval and consent to participate Not applicable.

Consent for publication Not applicable.

Competing interests The authors declare no competing interests.

References

1. Vitale I, Pietrocola F, Guilbaud E, Aaronson SA, Abrams JM, Adam D et al (2023) Apoptotic cell death in disease—Current Understanding of the NCCD 2023. Cell Death Differ 30:1097–1154. https://doi.org/10.1038/s41418-023-01153-w
2. Kerr JF, Wyllie AH (1972) Currie. Apoptosis: a basic biological phenomenon with wide-ranging implications in tissue kinetics. Br J Cancer 26:239–257. https://doi.org/10.1038/bjc.1972.33
3. Park W, Wei S, Kim B-S, Kim B, Bae S-J, Chae YC et al (2023) Diversity and complexity of cell death: a historical review. Exp Mol Med 55:1573–1594. https://doi.org/10.1038/s12276-023-01078-x
4. Lockshin RA (1964) Williams. Programmed cell death—II. Endocrine potentiation of the breakdown of the intersegmental muscles of silkmoths. J Insect Physiol 10:643–649. https://doi.org/10.1016/0022-1910(64)90034-4
5. Galluzzi L, Vitale I, Abrams JM, Alnemri ES, Baehrecke EH, Blagosklonny MV et al (2012) Molecular definitions of cell death subroutines: recommendations of the nomenclature committee on cell death 2012. Cell Death Differ 19:107–120. https://doi.org/10.1038/cdd.2011.96
6. Koopman G, Reutelingsperger CP, Kuijten GA, Keehnen RM, Pals ST, van Oers MH (1994) Annexin V for flow cytometric detection of phosphatidylserine expression on B cells undergoing apoptosis. Blood 84:1415–1420. https://doi.org/10.1182/blood.V84.5.1415.1415
7. Wilkins RC, Kutzner BC, Truong M, Sanchez-Dardon J, McLean JRN (2002) Analysis of radiation-induced apoptosis in human lymphocytes: flow cytometry using Annexin V and Propidium iodide versus the neutral comet assay. Cytometry 48:14–19. https://doi.org/10.1002/cyto.10098
8. Aubry J-P, Blaecke A, Lecoanet-Henchoz S, Jeannin P, Herbault N, Caron G et al (1999) Annexin V used for measuring apoptosis in the early events of cellular cytotoxicity. Cytometry 37:197–204. https://doi.org/10.1002/(SICI)1097-0320(19991101)37:3%3C197::AID-CYTO6%3E3.0.CO;2-L
9. Mohamed HRH, Elberry YA, Magdy H, Ismail M, Michael M, Eltayeb N et al (2025) Erbium oxide nanoparticles induce potent cell death, genomic instability and ROS-mitochondrial dysfunction-mediated apoptosis in U937 lymphoma cells. Naunyn Schmiedebergs Arch Pharmacol 398:11027–11039. https://doi.org/10.1007/s00210-025-03962-x
10. Mangal S, Jana S, Dutta A, Kar R, Are V, Pradhan S et al (2025) Antiproliferative effect of filopaludina bengalensis fluid inducing apoptosis-necroptosis synergy with Immunogenic remodelling in triple-negative breast cancer. Sci Rep 15:41864. https://doi.org/10.1038/s41598-025-25810-x
11. Solak K, Yildiz Arslan S, Acar M, Turhan F, Unver Y, Mavi A (2025) Combination of magnetic hyperthermia and gene therapy for breast cancer. Apoptosis 30:99–116. https://doi.org/10.1007/s10495-024-02026-4
12. Asgari F, Javani Jouni F, Zafari J, Sari S, Ashrafi P (2025) Enhanced effects of photodynamic therapy and celecoxib on the triple–negative breast cancer MDA–MB–231 cell line: impact on BCL–2, BAX, and TP53 gene expression. Photodiagn Photodyn Ther 56:105263. https://doi.org/10.1016/j.pdpdt.2025.105263

13. Asoudeh-Fard A, Jahromi HH, Zare Z, Fazlinia A, Nazari MB (2025) A. Parsaei. In vitro cytotoxic and pro-apoptotic effects of Chaetoceros socialis ethanolic extract on prostate (LNCap) and glioblastoma (U-87 MG) cells via modulation of AKT/PTEN, mTOR, BAX/BCL2, and Caspase pathways. *Medical oncology* 42 :488. https://doi.org/10.1007/s12032-025-03034-3
14. Haas B, Roth I, Säcker L, Wos-Maganga M, Beltzig L, Kaina B (2025) Apoptotic and senolytic effects of hERG/Eag1 channel blockers in combination with Temozolomide in human glioblastoma cells. Naunyn Schmiedebergs Arch Pharmacol. https://doi.org/10.1007/s00210-025-03955-w
15. Ziyabakhsh A, Vatankhah MA, Pakizeh F, Nosrat A, Sobhi P, Vakili Ojarood M et al (2025) Genistein exerts anti-proliferative effects by regulating apoptosis and Autophagy-Related genes and MicroRNAs in human urinary bladder neoplasm EJ138 cells: an experimental and bioinformatic study. Iran J Pharm Res 24:e157853. https://doi.org/10.5812/ijpr-157853
16. Salavatipour MS, Kouhbananinejad SM, Lashkari M, Bardsiri MS, Moghadari M, Kashani B et al (2023) Kermanian propolis induces apoptosis through upregulation of Bax/Bcl-2 ratio in acute myeloblastic leukemia cell line (NB4). J Cancer Res Ther 19:327–334. https://doi.org/10.4103/jcrt.jcrt_1084_21
17. Kong J, Zhang Y, Ju X, Wang B, Diao X, Li J et al (2024) Electrostimulation evokes Caspase-3-Activated fast cancer cell pyroptosis and its nuclear stress response pathways. Anal Chem 96:13438–13446. https://doi.org/10.1021/acs.analchem.4c01206
18. Sazonova EV, Chesnokov MS, Zhivotovsky B, Kopeina GS (2022) Drug toxicity assessment: cell proliferation versus cell death. Cell Death Discovery 8:417. https://doi.org/10.1038/s41420-022-01207-x
19. Ren L-w, Li W, Zheng X-j, Liu J-y, Yang Y-h, Li S et al (2022) Benzimidazoles induce concurrent apoptosis and pyroptosis of human glioblastoma cells via arresting cell cycle. Acta Pharmacol Sin 43:194–208. https://doi.org/10.1038/s41401-021-00752-y
20. El-Hajjar L, Ali Ahmad F (2023) Nasr. A guide to flow cytometry: components, basic principles, experimental design, and cancer research applications. Curr Protocols 3:e721. https://doi.org/10.1002/cpz1.721
21. D. M. Jameson. Perspectives on fluorescence: a tribute to Gregorio Weber: Springer; (2016) 1–16 p
22. Weber G (1952) Polarization of the fluorescence of macromolecules. 1. Theory and experimental method. Biochem J 51:145–155. https://doi.org/10.1042/bj0510145
23. Eisenstein M (2006) Divide and conquer. Nature 441:1179–1179. https://doi.org/10.1038/4411179a
24. Fulwyler MJ (1965) Electronic separation of biological cells by volume. Science 150:910–911. https://doi.org/10.1126/science.150.3698.910
25. Herzenberg LA, Parks D, Sahaf B, Perez O, Roederer M, Herzenberg LA (2002) The history and future of the fluorescence activated cell sorter and flow cytometry: a view from Stanford. Clin Chem 48:1819–1827. https://doi.org/10.1093/clinchem/48.10.1819
26. Brestoff JR (2023) Full spectrum flow cytometry in the clinical laboratory. Int J Lab Hematol 45:44–49. https://doi.org/10.1111/ijlh.14098
27. Bartkowiak D, Högner S, Baust H, Nothdurft W, Röttinger EM (1999) Comparative analysis of apoptosis in HL60 detected by annexin-V and fluorescein-diacetate. Cytometry 37:191–196. https://doi.org/10.1002/(SICI)1097-0320(19991101)37:3%3C191::AID-CYTO5%3E3.0.CO;2-U
28. Frey T (1997) Correlated flow cytometric analysis of terminal events in apoptosis reveals the absence of some changes in some model systems. Cytometry 28:253–263. https://doi.org/10.1002/(SICI)1097-0320(19970701)28:3%3C253::AID-CYTO10%3E3.0.CO;2-O
29. King MA, Radicchi-Mastroianni MA (2000) Wells. There is substantial nuclear and cellular disintegration before detectable phosphatidylserine exposure during the camptothecin-induced apoptosis of HL-60 cells. Cytometry 40:10–18. https://doi.org/10.1002/(SICI)1097-0320(20000501)40:1%3C10::AID-CYTO2%3E3.0.CO;2-F
30. Montgomery ST, Stick SM, Kicic A (2020) An adapted novel flow cytometry methodology to delineate types of cell death in airway epithelial cells. J Biol Methods 7. https://doi.org/10.14440/jbm.2020.336
31. Wallberg F, Tenev T, Meier P (2016) (2016):pdb.prot087387 Analysis of Apoptosis and Necroptosis by Fluorescence-Activated Cell Sorting. *Cold Spring Harbor Protocols* https://doi.org/10.1101/pdb.prot087387
32. van Engeland M, Nieland LJW, Ramaekers FCS, Schutte B (1998) Reutelingsperger. Annexin V-Affinity assay: a review on an apoptosis detection system based on phosphatidylserine exposure. Cytometry 31(19980101):1–9. https://doi.org/10.1002/(SICI)1097-0320.)31:1%3C1::AID-CYTO1%3E3.0.CO;2-R
33. Jones KH, Senft JA (1985) An improved method to determine cell viability by simultaneous staining with fluorescein diacetate-propidium iodide. J Histochem Cytochemistry 33:77–79. https://doi.org/10.1177/33.1.2578146
34. Krishan A (1975) Rapid flow cytofluorometric analysis of mammalian cell cycle by Propidium iodide staining. J Cell Biol 66:188–193. https://doi.org/10.1083/jcb.66.1.188
35. Inaba N, Sato N, Ijichi M, Fukazawa I, Nito A, Takamizawa H et al (1984) The immunocytochemical location of two membrane-associated placental tissue proteins in human and cynomolgus monkey placentae. Tumour Biol 5:75–85. https://pubmed.ncbi.nlm.nih.gov/6239364/
36. Reutelingsperger CPM, Hornstra G, Hemker HC (1985) Isolation and partial purification of a novel anticoagulant from arteries of human umbilical cord. Eur J Biochem 151:625–629. https://doi.org/10.1111/j.1432-1033.1985.tb09150.x
37. van Engeland M, Ramaekers FCS, Schutte B, Reutelingsperger CPM (1996) A novel assay to measure loss of plasma membrane asymmetry during apoptosis of adherent cells in culture. Cytometry 24(19960601):131–139. https://doi.org/10.1002/(SICI)1097-0320.)24:2%3C131::AID-CYTO5%3E3.0.CO;2-M
38. Crissman HA (1973) Steinkamp. Rapid, simultaneous measurement of DNA, protein, and cell volume in single cells from large mammalian cell populations. J Cell Biol 59:766–771. https://doi.org/10.1083/jcb.59.3.766
39. Martens ACM, van den Engh GJ, Hagenbeek A (1981) The fluorescence intensity of Propidium iodide bound to DNA depends on the concentration of sodium chloride. Cytometry 2:24–25. https://doi.org/10.1002/cyto.990020105
40. Vindeløv LL (1977) Flow microfluorometric analysis of nuclear DNA in cells from solid tumors and cell suspensions: a new method for rapid isolation and staining of nuclei. Virchows Archiv B 24:227–242. https://doi.org/10.1007/BF02889282
41. Deitch AD, Law H, deVere R, White (1982) A stable Propidium iodide staining procedure for flow cytometry. J Histochem Cytochemistry 30:967–972. https://doi.org/10.1177/30.9.6182188
42. Span LFR, Pennings AHM, Vierwinden G, Boezeman JBM, Raymakers RAP, de Witte T (2002) The dynamic process of apoptosis analyzed by flow cytometry using Annexin-V/propidium iodide and a modified in situ end labeling technique. Cytometry 47:24–31. https://doi.org/10.1002/cyto.10028
43. Henery S, George T, Hall B, Basiji D, Ortyn W, Morrissey P (2008) Quantitative image based apoptotic index measurement using multispectral imaging flow cytometry: a comparison with standard photometric methods. Apoptosis 13:1054–1063. https://doi.org/10.1007/s10495-008-0227-4

44. Bacsó Z, Everson RB (2000) Eliason. The DNA of Annexin V-binding apoptotic cells is highly Fragmented1. Cancer Res 60:4623–4628
45. Salim EI, Alabasy MM, Nashar EME, Al-Zahrani NS, Alzahrani MA, Guo Z et al (2024) Molecular interactions between Metformin and D-limonene inhibit proliferation and promote apoptosis in breast and liver cancer cells. BMC Complement Med Ther 24:185. https://doi.org/10.1186/s12906-024-04453-x
46. Baeza-Morales A, Pascual-García S, Martínez-Peinado P, Navarro-Sempere A, Segovia Y, Medina-García M et al (2025) Bacterioruberin extract from haloferax mediterranei induces apoptosis and cell cycle arrest in myeloid leukaemia cell lines. Sci Rep 15:23485. https://doi.org/10.1038/s41598-025-06999-3
47. Kim IY, Kwak M, Kim J, Lee TG (2022) Heo. Comparative study on nanotoxicity in human primary and cancer cells. Nanomaterials [Internet] 12(6):993
48. Yong J, von Bremen J, Groeger S, Ruiz-Heiland G, Ruf S (2021) Hypoxia-inducible factor 1-alpha acts as a Bridge factor for cross-talk between ERK1/2 and caspases in hypoxia-induced apoptosis of cementoblasts. J Cell Mol Med 25:9710–9723. https://doi.org/10.1111/jcmm.16920
49. Liu M, Li H, Yang R, Ji D, Xia X (2022) GSK872 and necrostatin-1 protect retinal ganglion cells against necroptosis through Inhibition of RIP1/RIP3/MLKL pathway in glutamate-induced retinal excitotoxic model of glaucoma. J Neuroinflamm 19:262. https://doi.org/10.1186/s12974-022-02626-4
50. Li J, Tang M, Ke R-X, Li P-L, Sheng Z-G (2024) Zhu. The anticancer drug candidate CBL0137 induced necroptosis via forming left-handed Z-DNA and its binding protein ZBP1 in liver cells. Toxicol Appl Pharmcol 482:116765. https://doi.org/10.1016/j.taap.2023.116765
51. Parvaneh S, Pourmadadi M, Abdouss M, Pourmousavi SA, Yazdian F, Rahdar A et al (2023) Carboxymethyl cellulose/starch/reduced graphene oxide composite as a pH-sensitive nanocarrier for Curcumin drug delivery. Int J Biol Macromol 241:124566. https://doi.org/10.1016/j.ijbiomac.2023.124566
52. Rogers C, Fernandes-Alnemri T, Mayes L, Alnemri D, Cingolani G (2017) Alnemri. Cleavage of DFNA5 by caspase-3 during apoptosis mediates progression to secondary necrotic/pyroptotic cell death. Nat Commun 8:14128. https://doi.org/10.1038/ncomms14128
53. Mikaeili Ghezeljeh S, Salehzadeh A, Ataei-e S, Jaliseh (2024) Iron oxide nanoparticles coated with glucose and conjugated with Safranal (Fe3O4@Glu-Safranal NPs) inducing apoptosis in liver cancer cell line (HepG2). BMC Chem 18:33. https://doi.org/10.1186/s13065-024-01142-1
54. Wallberg F, Tenev T, Meier P (2016) (2016):pdb.prot087395 Time-Lapse Imaging of Cell Death. *Cold Spring Harbor Protocols* https://doi.org/10.1101/pdb.prot087395
55. Jiang S, Qin K, Sun L (2023) Time-lapse live-cell imaging of pyroptosis by confocal microscopy. STAR Protocols 4:102708. https://doi.org/10.1016/j.xpro.2023.102708
56. Wållberg F, Tenev T, Meier P (2013) Time-Lapse imaging of necrosis. In: McCall K, Klein C (eds) Necrosis: methods and Protocols. 1004. Humana, Totowa, NJ, pp 17–29. https://doi.org/10.1007/978-1-62703-383-1_2.
57. Qiu Y, Hüther JA, Wank B, Rath A, Tykwe R, Aldrovandi M et al (2025) Interplay of ferroptotic and apoptotic cell death and its modulation by BH3-mimetics. Cell Death Differ. https://doi.org/10.1038/s41418-025-01514-7
58. Jiang L, Tixeira R, Caruso S, Atkin-Smith GK, Baxter AA, Paone S et al (2016) Monitoring the progression of cell death and the disassembly of dying cells by flow cytometry. Nat Protoc 11:655–663. https://doi.org/10.1038/nprot.2016.028
59. Jiang L, Paone S, Caruso S, Atkin-Smith GK, Phan TK, Hulett MD et al (2017) Determining the contents and cell origins of apoptotic bodies by flow cytometry. Sci Rep 7:14444. https://doi.org/10.1038/s41598-017-14305-z
60. Lee SH, Meng XW, Flatten KS, Loegering DA (2013) Kaufmann. Phosphatidylserine exposure during apoptosis reflects bidirectional trafficking between plasma membrane and cytoplasm. Cell Death Differ 20:64–76. https://doi.org/10.1038/cdd.2012.93
61. Fadeel B, Gleiss B, Högstrand K, Chandra J, Wiedmer T, Sims PJ et al (1999) Phosphatidylserine exposure during apoptosis is a Cell-Type-Specific event and does not correlate with plasma membrane phospholipid scramblase expression. Biochem Bioph Res Co 266:504–511. https://doi.org/10.1006/bbrc.1999.1820
62. Yevale D, Buha V, Sangani DU, Teraiya N, Sangani CB, Patel N (2025) Novel anticancer inhibitors targeting the PI3K/Akt/mTOR signaling route and apoptosis inducers: a study on the apoptosis mechanism via the intrinsic mitochondrial-mediated pathway. Chemico-Biol Interact 419:111635. https://doi.org/10.1016/j.cbi.2025.111635
63. Krysko O, De Ridder L, Cornelissen M (2004) Phosphatidylserine exposure during early primary necrosis (oncosis) in JB6 cells as evidenced by Immunogold labeling technique. Apoptosis 9:495–500. https://doi.org/10.1023/b:appt.0000031452.75162.75
64. Filho AM, Laversanne M, Ferlay J, Colombet M, Piñeros M, Znaor A et al (2025) The GLOBOCAN 2022 cancer estimates: data sources, methods, and a snapshot of the cancer burden worldwide. Int J Cancer 156:1336–1346. https://doi.org/10.1002/ijc.35278
65. Berda-Haddad Y, Robert S, Salers P, Zekraoui L, Farnarier C, Dinarello CA et al (2011) Sterile inflammation of endothelial cell-derived apoptotic bodies is mediated by interleukin-1α. *Proceedings of the National Academy of Sciences* 108 :20684–20689. https://doi.org/10.1073/pnas.1116848108
66. Gary A-S (2020) Rochette. Apoptosis, the only cell death pathway that can be measured in human diploid dermal fibroblasts following lethal UVB irradiation. Sci Rep 10:18946. https://doi.org/10.1038/s41598-020-75873-1
67. Diaz Sanchez L, Sanchez-Aranguren L, Wang K, Spickett CM, Griffiths HR (2023) Dias. TNF-α-Mediated endothelial cell apoptosis is rescued by hydrogen sulfide. Antioxid (Basel Switzerland) 12:734. https://doi.org/10.3390/antiox12030734
68. Galluzzi L, Vitale I, Aaronson SA, Abrams JM, Adam D, Agostinis P et al (2018) Molecular mechanisms of cell death: recommendations of the nomenclature committee on cell death 2018. Cell Death Differ 25:486–541. https://doi.org/10.1038/s41418-017-0012-4
69. Luo R, Yang Y, Zhang Y, Xue X, Guo M, Li X (2025) Mitochondrial damage-associated molecular patterns (mito-DAMPs): determinants of hepatopathy progression and therapeutic implications. Pharmacol Res 221:107980. https://doi.org/10.1016/j.phrs.2025.107980
70. Xu G, Chen S, Yang H, Feng X, Li F, Zhao H et al (2025) An ER stress and mitochondrial apoptosis Co-inducer for enhanced cancer immunotherapy. Cancer Lett 612:217485. https://doi.org/10.1016/j.canlet.2025.217485
71. Terraza-Silvestre E, Villamuera R, Bandera-Linero J, Letek M, Oña-Sánchez D, Ramón-Barros C et al (2025) An unconventional autophagic pathway that inhibits ATP secretion during apoptotic cell death. Nat Commun 16:3409. https://doi.org/10.1038/s41467-025-58619-3
72. Ganci D, D'Anna L, Abruscato G, Le Chevalier M, Quideau O, Cataldo S et al (2025) Harnessing redox reactions for anticancer effects: a copper(II) schiff base complex induces apoptosis in HepG2 liver cancer cells via ROS generation. J Inorg Biochem 270:112938. https://doi.org/10.1016/j.jinorgbio.2025.112938
73. Li H, Ouyang J, Wang X, Qian C (2025) Platycodin D enhances glioma sensitivity to Temozolomide by Inhibition of the

Wnt/β-Catenin pathway. Drug Des Devel Ther 19:1811–1824. https://doi.org/10.2147/DDDT.S503167
74. Esnaashari F, Zamani H, Zahmatkesh H, Soleimani M, Dashtaki GA, Rasti B (2025) Berberine decorated zinc oxide loaded Chitosan nanoparticles a potent anti cancer agent against breast cancer. Sci Rep 15:3185. https://doi.org/10.1038/s41598-025-87445-2
75. Balusamy SR, Samad A, Singh P, Sunderraj S, Elsadek MF, Altwaijry N et al (2025) Comparative anti-cancer properties of carene isoforms induced apoptotic cell death in stomach and lung cancer cell lines. Naunyn Schmiedebergs Arch Pharmacol. https://doi.org/10.1007/s00210-025-04380-9
76. Bae Y, Seo J, Jeong W (2024) P53 genotype-independent anticancer effects of olibanum extract and 11-keto-beta-boswellic acid on human colorectal cancer cells. Phytomedicine Plus 4:100641. https://doi.org/10.1016/j.phyplu.2024.100641
77. Zhuang X, Yao J, Li X, Jiang Y, Zhong M, Tan J et al (2024) Anlotinib suppresses the DNA damage response by disrupting SETD1A and inducing p53-dependent apoptosis in transformed follicular lymphoma. Int J Med Sci 21:70–79. https://doi.org/10.7150/ijms.84952
78. Fadayomi IE, Johnson-Ajinwo OR, Pires E, McCullagh J, Claridge TDW, Forsyth NR et al (2021) Clerodane diterpenoids from an edible plant Justicia insularis: discovery, Cytotoxicity, and apoptosis induction in human ovarian cancer cells. Molecules 26:5933. https://doi.org/10.3390/molecules26195933
79. Qu Y, Zhao J, Ma L, Wang X, Sun F, Li Y et al (2025) Intranasal delivery of Temozolomide and Disulfiram in situ gel combined with copper for enhanced glioblastoma therapy. Colloids Surf B 255:114898. https://doi.org/10.1016/j.colsurfb.2025.114898
80. Ding Y, Chen X, Liu C, Ge W, Wang Q, Hao X et al (2021) Identification of a small molecule as inducer of ferroptosis and apoptosis through ubiquitination of GPX4 in triple negative breast cancer cells. J Hematol Oncol 14:19. https://doi.org/10.1186/s13045-020-01016-8
81. Wu X, Pang J, Li W, Jia X, Zhang Z, Jiang M et al (2025) Development a stannum(IV) 8-quinolinecarbaldehyde thiosemicarbazone complex with remarkable anticancer activity via pyroptosis and apoptosis. J Mol Struct 1337:142225. https://doi.org/10.1016/j.molstruc.2025.142225
82. Huang N, Feng Y, Liu Y, Zhang Y, Liu L, Zhang B et al (2024) Disulfiram mediated anti-tumour effect in pituitary neuroendocrine tumours by inducing Cuproptosis. Int Immunopharmacol 134:112159. https://doi.org/10.1016/j.intimp.2024.112159
83. Putri HE, Sae-Fung A, Lomphithak T, Jitkaew S (2025) Kaempferol enhances Immunogenic cell death via Premortem stress and necroptosis in cholangiocarcinoma: insights from network Pharmacology and mechanistic studies. Comput Biol Med 195:110646. https://doi.org/10.1016/j.compbiomed.2025.110646
84. Zhong C, Wang S, Zhang J, Zheng Q, Lei Y, Xu Y et al (2025) Deoxypodophyllotoxin inhibited the growth of malignant pleural mesothelioma by inducing necroptosis and mitotic catastrophe. Phytomedicine 143:156786. https://doi.org/10.1016/j.phymed.2025.156786
85. Wang P, Zheng S-Y, Jiang R-L, Wu H-D, Li Y-A, Lu J-L et al (2023) Necroptosis signaling and mitochondrial dysfunction cross-talking facilitate cell death mediated by chelerythrine in glioma. Free Radic Biol Med 202:76–96. https://doi.org/10.1016/j.freeradbiomed.2023.03.021
86. He K, Ding B, Li J, Meng Q, Chen H, Li Z et al (2025) Oxamate nanoparticles for enhanced tumor immunotherapy through blocking Glycolysis metabolism and inducing pyroptosis. Nano Lett 25:10053–10062. https://doi.org/10.1021/acs.nanolett.5c01811
87. Hao X, Tang Y, Xu W, Wang M, Liu J, Li Y et al (2025) Engineered biomimetic cisplatin-polyphenol nanocomplex for chemo-immunotherapy of glioblastoma by inducing pyroptosis. J Nanobiotechnol 23:14. https://doi.org/10.1186/s12951-025-03091-w
88. Zhao X, Chen C, Han W, Liang M, Cheng Y, Chen Y et al (2024) EEBR induces Caspase-1-dependent pyroptosis through the NF-κB/NLRP3 signalling cascade in non-small cell lung cancer. J Cell Mol Med n/a. https://doi.org/10.1111/jcmm.18094
89. Upadhyay S, Ahmad R, Ghildiyal S, Baluni M, Singh A, Husain I et al (2025) Anticancer potential of allium sativum against triple-negative breast cancer cells: evidence from ROS-mediated cell cycle arrest and apoptosis. South Afr J Bot 179:31–38. https://doi.org/10.1016/j.sajb.2025.01.039
90. Zeng D, Li K, Xing A, Wang J, Hao Y, Zhang Z et al (2025) Novel naringenin hydrazone derivatives: synthesis, characterization, antioxidant and antitumor activity evaluation. J Mol Struct 1348:143435. https://doi.org/10.1016/j.molstruc.2025.143435
91. Bendale Y, Bendale V, Paul S (2017) Evaluation of cytotoxic activity of platinum nanoparticles against normal and cancer cells and its anticancer potential through induction of apoptosis. Integr Med Res 6:141–148. https://doi.org/10.1016/j.imr.2017.01.006
92. Guo J, Xu B, Han Q, Zhou H, Xia Y, Gong C et al (2018) Ferroptosis: a novel Anti-tumor action for cisplatin. Cancer Res Treatment: Official J Korean Cancer Association 50:445–460. https://doi.org/10.4143/crt.2016.572
93. Birsen R, Larrue C, Decroocq J, Johnson N, Guiraud N, Gotanegre M et al (2022) APR-246 induces early cell death by ferroptosis in acute myeloid leukemia. Haematologica 107:403–416. https://doi.org/10.3324/haematol.2020.259531
94. Chen X, Wang Z, Li C, Zhang Z, Lu S, Wang X et al (2024) SIRT1 activated by AROS sensitizes glioma cells to ferroptosis via induction of NAD+depletion-dependent activation of ATF3. Redox Biol 69:103030. https://doi.org/10.1016/j.redox.2024.103030
95. Zhang Z, Ji Y, Hu N, Yu Q, Zhang X, Li J et al (2022) Ferroptosis-induced anticancer effect of Resveratrol with a biomimetic nanodelivery system in colorectal cancer treatment. Asian J Pharm Sci 17:751–766. https://doi.org/10.1016/j.ajps.2022.07.006
96. Shao K-Y, Luo S-D, Huang E-Y, Chang T-M, Botcha L, Sehar M et al (2025) Acetylshikonin induces cell necroptosis via mediating mitochondrial function and oxidative stress-regulated signaling in human oral cancer cells. Bioorg Chem 159:108396. https://doi.org/10.1016/j.bioorg.2025.108396
97. Wang Z, Tang Y, Li Q (2025) A self-assembling nanoplatform for pyroptosis and ferroptosis enhanced cancer photoimmunotherapy. Light: Sci Appl 14:16. https://doi.org/10.1038/s41377-024-01673-1
98. Song F, Wei L, Wu J, Zhu G, Zhang J, Li H (2025) Plumbagin activates NLRP3/caspase-1/GSDMD-mediated pyroptosis by decreasing DUSP4 expression to exhibit anticancer property in cholangiocarcinoma. Toxicol Appl Pharmcol 117492. https://doi.org/10.1016/j.taap.2025.117492
99. Yang C, Wang Z-Q, Zhang Z-C, Lou G, Jin W-L (2023) CBL0137 activates ROS/BAX signaling to promote caspase-3/GSDME-dependent pyroptosis in ovarian cancer cells. Biomed Pharmacother 161:114529. https://doi.org/10.1016/j.biopha.2023.114529
100. Chang Y, Li Y, Ye N, Guo X, Li Z, Sun G et al (2016) Atorvastatin inhibits the apoptosis of human umbilical vein endothelial cells induced by angiotensin II via the lysosomal-mitochondrial axis. Apoptosis 21:977–996. https://doi.org/10.1007/s10495-016-1271-0
101. Atsumi T, Tonosaki K, Fujisawa S Induction of early apoptosis and ROS-generation activity in human gingival fibroblasts (HGF) and human submandibular gland carcinoma (HSG) cells treated with Curcumin. Arch Oral Biol 51 (2006):913–921. https://doi.org/10.1016/j.archoralbio.2006.03.016
102. He A-E, Wang X, Xie N (2025) Xiao. ZBP1-NLRP3 axis integrates PANoptosis and ferroptosis during inflammatory injury in

human dental pulp fibroblasts. Arch Oral Biol 180:106398. https://doi.org/10.1016/j.archoralbio.2025.106398
103. Liu W, Liu J, Wang W, Wang Y, Ouyang X (2018) NLRP6 induces pyroptosis by activation of Caspase-1 in gingival fibroblasts. J Dent Res 97:1391–1398. https://doi.org/10.1177/0022034518775036
104. Wiernicki B, Maschalidi S, Pinney J, Adjemian S, Vanden Berghe T, Ravichandran KS et al (2022) Cancer cells dying from ferroptosis impede dendritic cell-mediated anti-tumor immunity. Nat Commun 13:3676. https://doi.org/10.1038/s41467-022-31218-2
105. Herault O, Colombat P, Domenech J, Degenne M, Bremond JL, Sensebe L et al (1999) A rapid single-laser flow cytometric method for discrimination of early apoptotic cells in a heterogenous cell population. Brit J Haematol 104:530–537. https://doi.org/10.1046/j.1365-2141.1999.01203.x
106. Bi M-C, Rosen R, Zha R-Y, McCormick SA, Song E, Hu D-N (2013) Zeaxanthin induces apoptosis in human uveal melanoma cells through Bcl-2 family proteins and intrinsic apoptosis pathway. Evidence-Based Complement Altern Med 2013:205082. https://doi.org/10.1155/2013/205082
107. Martínez-Rodrigo L, Gacem S, Brüggemann M, Pinto S, Mocé E, Serrano-Jara D et al (2025) Evaluating DAPI stain to assess sperm membrane integrity by flow cytometry in livestock species. Vet Res Commun 49:357. https://doi.org/10.1007/s11259-025-10948-w
108. Schmid I, Krall WJ, Uittenbogaart CH, Braun J (1992) Giorgi. Dead cell discrimination with 7-amino-actinomcin D in combination with dual color Immunofluorescence in single laser flow cytometry. Cytometry 13:204–208. https://doi.org/10.1002/cyto.990130216
109. Falzone N, Huyser C, Franken DR (2010) Comparison between Propidium iodide and 7-amino-actinomycin-D for viability assessment during flow cytometric analyses of the human sperm acrosome. Andrologia 42:20–26. https://doi.org/10.1111/j.1439-0272.2009.00949.x
110. Hasper HJ, Weghorst RM, Richel DJ, Meerwaldt JH, Olthuis FMFG (2000) I. Schenkeveld. A new four-color flow cytometric assay to detect apoptosis in lymphocyte subsets of cultured peripheral blood cells. Cytometry 40:167–171. https://doi.org/10.1002/(SICI)1097-0320(20000601)40:2%3C167::AID-CYTO11%3E3.0.CO;2-1
111. Pang X, Fu C, Chen J, Su M, Wei R, Wang Y et al (2023) A manganese-phenolic network platform amplifying STING activation to potentiate MRI guided cancer chemo-/chemodynamic/immune therapy. Biomaterials Sci 11:3840–3850. https://doi.org/10.1039/D2BM02140D
112. Uhl KL, Schultz CR, Geerts D (2018) Bachmann. Harmine, a dual-specificity tyrosine phosphorylation-regulated kinase (DYRK) inhibitor induces caspase-mediated apoptosis in neuroblastoma. Cancer Cell Int 18:82. https://doi.org/10.1186/s12935-018-0574-3
113. Huang L-l, Long R-t, Jiang G-p, Jiang X, Sun H, Guo H et al (2018) Augmenter of liver regeneration promotes mitochondrial biogenesis in renal ischemia–reperfusion injury. Apoptosis 23:695–706. https://doi.org/10.1007/s10495-018-1487-2
114. Wang L, Huang Y, Zhang X, Chen W, Dai Z (2025) Exosomes derived from FN14-overexpressing BMSCs activate the NF-κB signaling pathway to induce PANoptosis in osteosarcoma. Apoptosis 30:880–893. https://doi.org/10.1007/s10495-024-02071-z
115. Alshehade SA, Almoustafa HA, Alshawsh MA, Chik Z (2024) Flow cytometry-based quantitative analysis of cellular protein expression in apoptosis subpopulations: a protocol. Heliyon 10:e33665. https://doi.org/10.1016/j.heliyon.2024.e33665
116. Henry CM, Hollville E, Martin SJ (2013) Measuring apoptosis by microscopy and flow cytometry. Methods 61:90–97. https://doi.org/10.1016/j.ymeth.2013.01.008
117. Rieger AM, Nelson KL, Konowalchuk JD (2011) Barreda. Modified Annexin V/propidium iodide apoptosis assay for accurate assessment of cell death. J Visualised Experiments 2597. https://doi.org/10.3791/2597
118. Wlodkowic D, Skommer J (2009) Z. Darzynkiewicz. Flow Cytometry-Based Apoptosis Detection. In: Erhardt P, Toth A, editors. Apoptosis: methods and protocols, Second Edition. Totowa, NJ: Humana Press; pp. 19–32. https://doi.org/10.1007/978-1-60327-017-5_2
119. Costigan A, Hollville E, Martin SJ (2023) Discriminating between Apoptosis, Necrosis, Necroptosis, and ferroptosis by microscopy and flow cytometry. Curr Protocols 3:e951. https://doi.org/10.1002/cpz1.951
120. Lee HL, Pike R, Chong MHA, Vossenkamper A, Warnes G (2018) Simultaneous flow cytometric immunophenotyping of necroptosis, apoptosis and RIP1-dependent apoptosis. Methods 134–135. https://doi.org/10.1016/j.ymeth.2017.10.013
121. Chen Y, Li X, Yang M, Liu S-B (2024) Research progress on morphology and mechanism of programmed cell death. Cell Death Dis 15:327. https://doi.org/10.1038/s41419-024-06712-8
122. Tong X, Tang R, Xiao M, Xu J, Wang W, Zhang B et al (2022) Targeting cell death pathways for cancer therapy: recent developments in necroptosis, pyroptosis, ferroptosis, and Cuproptosis research. J Hematol Oncol 15:174. https://doi.org/10.1186/s13045-022-01392-3
123. Gielecińska A, Kciuk M, Yahya EB, Ainane T, Mujwar S, Kontek R (2023) Apoptosis, necroptosis, and pyroptosis as alternative cell death pathways induced by chemotherapeutic agents? Biochim Et Biophys Acta (BBA) - Reviews Cancer 1878:189024. https://doi.org/10.1016/j.bbcan.2023.189024
124. Ning J, Chen L, Zeng Y, Xiao G, Tian W, Wu Q et al (2024) The scheme, and regulative mechanism of pyroptosis, ferroptosis, and necroptosis in radiation injury. Int J Biol Sci 20:1871–1883. https://doi.org/10.7150/ijbs.91112
125. Dharavath A, Kaur S, Mohan PVD, Guru SK (2025) Harnessing cuproptosis: a new avenue for targeted cancer therapies. Apoptosis. https://doi.org/10.1007/s10495-025-02174-1
126. Khalef L, Lydia R, Filicia K, Moussa B (2024) Cell viability and cytotoxicity assays: biochemical elements and cellular compartments. Cell Biochem Funct 42:e4007. https://doi.org/10.1002/cbf.4007
127. Tenev T, Bianchi K, Darding M, Broemer M, Langlais C, Wallberg F et al (2011) The Ripoptosome, a signaling platform that assembles in response to genotoxic stress and loss of IAPs. Mol Cell 43:432–448. https://doi.org/10.1016/j.molcel.2011.06.006
128. Liang S, Lv ZT, Zhang JM, Wang YT, Dong YH, Wang ZG et al (2018) Necrostatin-1 attenuates Trauma-Induced mouse osteoarthritis and IL-1β induced apoptosis via HMGB1/TLR4/SDF-1 in primary mouse chondrocytes. Front Pharmacol 9:1378. https://doi.org/10.3389/fphar.2018.01378
129. Wang Y-Q, Wang L, Zhang M-Y, Wang T, Bao H-J, Liu W-L et al (2012) Necrostatin-1 suppresses autophagy and apoptosis in mice traumatic brain injury model. Neurochem Res 37:1849–1858. https://doi.org/10.1007/s11064-012-0791-4
130. Lin CY, Chang TW, Hsieh WH, Hung MC, Lin IH, Lai SC et al (2016) Simultaneous induction of apoptosis and necroptosis by Tanshinone IIA in human hepatocellular carcinoma HepG2 cells. Cell Death Discovery 2:16065. https://doi.org/10.1038/cddiscovery.2016.65
131. Sawai H, Domae N (2011) Discrimination between primary necrosis and apoptosis by necrostatin-1 in Annexin V-positive/propidium iodide-negative cells. Biochem Bioph Res Co 411:569–573. https://doi.org/10.1016/j.bbrc.2011.06.186
132. Rojas-Rivera D, Beltrán S, Muñoz-Carvajal F, Ahumada-Montalva P, Abarzúa L, Gomez L et al (2024) The autophagy protein RUBCNL/PACER represses RIPK1 kinase-dependent apoptosis

and necroptosis. Autophagy 20:2444–2459. https://doi.org/10.1080/15548627.2024.2367923
133. Kelepouras K, Saggau J, Varanda AB, Zrilic M, Kiefer C, Rakhsh-Khorshid H et al (2024) The importance of murine phospho-MLKL-S345 in situ detection for necroptosis assessment in vivo. Cell Death Differ 31:897–909. https://doi.org/10.1038/s41418-024-01313-6
134. Gary A-S, Amouret S, Montoni A (2024) Rochette. MLKL, a new actor of UVB-induced apoptosis in human diploid dermal fibroblasts. Cell Death Discovery 10:232. https://doi.org/10.1038/s41420-024-02004-4
135. Berghe TV, Vanlangenakker N, Parthoens E, Deckers W, Devos M, Festjens N et al (2010) Necroptosis, necrosis and secondary necrosis converge on similar cellular disintegration features. Cell Death Differ 17:922–930. https://doi.org/10.1038/cdd.2009.184
136. Qu X, Zou Z, Sun Q, Luby-Phelps K, Cheng P, Hogan RN et al (2007) Autophagy Gene-Dependent clearance of apoptotic cells during embryonic development. Cell 128:931–946. https://doi.org/10.1016/j.cell.2006.12.044
137. Wang Z, Hu H, Heitink L, Rogers K, You Y, Tan T et al (2023) The anti-cancer agent APR-246 can activate several programmed cell death processes to kill malignant cells. Cell Death Differ 30:1033–1046. https://doi.org/10.1038/s41418-023-01122-3
138. Jiao D, Cai Z, Choksi S, Ma D, Choe M, Kwon H-J et al (2018) Necroptosis of tumor cells leads to tumor necrosis and promotes tumor metastasis. Cell Res 28:868–870. https://doi.org/10.1038/s41422-018-0058-y
139. Pollard DA, Pollard TD (2019) Pollard. Empowering statistical methods for cellular and molecular biologists. Mol Biol Cell 30:1359–1368. https://doi.org/10.1091/mbc.E15-02-0076
140. Sun B, Luo J, Li Z, Chen D, Wang Q, Si W (2024) Muscone alleviates neuronal injury via increasing stress granules formation and reducing apoptosis in acute ischemic stroke. Exp Neurol 373:114678. https://doi.org/10.1016/j.expneurol.2024.114678
141. Ma J, Tian Y, Du C, Zhu Y, Huang W, Ding C et al (2025) Cerium-doped Prussian blue biomimetic nanozyme as an amplified pyroptosis inhibitor mitigate Aβ oligomer-induced neurotoxicity in alzheimer's disease. J Nanobiotechnol 23:181. https://doi.org/10.1186/s12951-025-03263-8